ELSEVIER

Journal of Molecular Catalysis A: Chemical 182–183 (2002) 227–238

JOURNAL OF MOLECULAR CATALYSIS A: CHEMICAL

www.elsevier.com/locate/molcata

Liquid-phase hydrogenation of hexadienes on metallic colloidal nanoparticles immobilized on supports via coordination capture by bifunctional organic molecules

Roberta Brayner, Guillaume Viau, François Bozon-Verduraz*

Laboratoire de Chimie des Matériaux Divisés et Catalyse, ITODYS, Université Paris 7, Case 7090, 2 Place Jussieu, 75251 Paris Cedex 05, France

Received 5 July 2001; accepted 29 October 2001

Abstract

Colloidal Pd, Ru and Pd–Cu are prepared in polyol solution (propane-1,2-diol) by either steric stabilization via poly(*N*-vinyl-2-pyrrolidone) (PVP) or electrostatic stabilization. The coordination capture is carried out with γ-mercaptopropyltriethoxysilane (γ-MPS) and 3-aminopropyltriethoxysilane (3-APS) previously grafted on the Nb_2O_5 and Al_2O_3 supports via the silane group. After interaction of the colloidal solutions with the grafted support, the immobilization yield is nearly 100% in the case of electrostatic stabilization but lower for steric stabilization. All catalysts present a very good global selectivity in the liquid-phase hydrogenation of hexa-1,5-diene (selectivity to hexenes). The PVP-protected samples present an initial induction time (30–50 min) due to the partial elimination of PVP by the solvent (*n*-heptane). The activity and hex-1-ene productivity of immobilized Pd samples are higher than those of unsupported colloidal Pd and immobilized Ru. This promising method, which avoids direct metal–support interactions, offer new possibilities to control the shape, size and structure of metal nanosized particles in a colloidal form, without change upon heterogenation.

Keywords: Colloidal particles; Immobilization; Nb_2O_5; Hexa-1,5-diene liquid-phase hydrogenation; Palladium; Ruthenium

1. Introduction

Much attention has recently been paid to the catalytic properties of unsupported metal clusters or colloids [1–4]; their study is of importance for understanding quantum size effects and relationship between homogeneous and heterogeneous catalysts. However, the separation of the catalytic system often raises serious problems and heterogenation procedures are relevant. In this work, a novel route is proposed: the immobilization of colloidal nanosized metal particles on supports via bifunctional and dis-symmetrical organic chains. This process, which was recently used for the fixation of nucleic acids onto various solids with application in medicine diagnostics [5], was aimed at the detection and quantification of chemical molecules, e.g. urea or cholesterol, or biological molecules like proteins, DNA or RNA [5–9].

Colloidal metal particles were recently immobilized from aqueous solution onto the surface of supports via: (i) a copolymer of polyacrylic acid (PAA) and polyethyleneimine [10]; (ii) a polyacrylamide gel (containing amino groups) and poly(*N*-vinyl-2-pyrrolidone) (PVP)-protected colloidal Pt [11]; (iii) hydrogen bonding between PAA and the polymers (e.g. PVP and polyvinyl alcohol, PVA) protecting the metal

* Corresponding author. Tel.: +33-1-44-27-5586; fax: +33-1-44-27-6137.
E-mail address: bozonver@ccr.jussieu.fr (F. Bozon-Verduraz).

1381-1169/02/$ – see front matter
PII: S1381-1169(01)00469-1

particles [12]; (iv) PVP or PVA with addition of formic acid, acetic acid or oxalic acid [13]. These catalysts were employed in the hydrogenation of alkenes, *cis*-cycloocta-1,5-diene, cyclopentadiene, cyclohexene, *o*-chloronitrobenzene and citronellal [10–13].

It was previously shown that the simple electrostatic adsorption of colloidal particles onto an ion-exchange resin, for example, leads to a rapid drop of catalytic activity resulting from the agglomeration of metal particles on the support surface due to Coulombic attraction [14].

The adsorption of polymers such as polyethylene oxide, cationic polymers, proteins and PVP on silica has been extensively studied [15]; in this paper, we apply the immobilization of mono- and bimetallic colloidal particles from polyol solutions onto Nb_2O_5 and Al_2O_3 via coordination capture by bifunctional organic molecules γ-mercaptopropyltriethoxysilane (γ-MPS) and 3-aminopropyltriethoxysilane (3-APS).

2. Experimental

Nb_2O_5 (HY-340) was supplied by CBMM (Companhia Brasileira de Metalurgia e Mineração, Brazil), palladium salts were obtained from Engelhard, France, and the γ-MPS and 3-APS were purchased from Aldrich.

Pd, Ru and Pd–Cu colloidal solutions are prepared in a polyol solution either by steric stabilization via PVP protection or by electrostatic stabilization [16]. The colloidal particles were obtained through direct reduction of Pd nitrate, Cu acetate and Ru chloride in a polyol solution at desired temperature with addition of PVP (Pd and PdCu colloidal particles) or of sodium acetate (Ru colloidal particles). The coordination capture was carried out with γ-MPS previously grafted on the Nb_2O_5 support via the silane group. The interaction of the colloidal metals with the grafted support is carried out through vigorous stirring at 60 °C for 6 h. After filtration, the immobilization yield is nearly 100% in the case of electrostatic stabilization but lower for steric stabilization.

Chemical analyses were carried out at the Materials Engineering Department, DEMAR/FAENQUIL, Lorena SP, Brazil, by inductively coupling plasma atomic emission spectroscopy (ICP-AES).

Powder X-ray diffraction (XRD) patterns were recorded using Co Kα radiation. The diffractometer was calibrated using a standard Si sample. The counting time was 30 s per step (2θ) of 0.05°. The mean crystallite size was estimated using the Scherrer equation, after computer fitting using a pseudo-Voigt function (software Profile-SOCABIM Diffract-At).

TEM measurements were performed with a JEOL 100 CXII microscope operating at 100 kV. The particle size distribution was obtained from the TEM pictures using a digital camera and the SAISAM and TAMIS software (Microvision Instruments), calculating the surface average particle diameter from $d_P = \sum n_i d_i^2 / \sum n_i d_i$.

Energy-dispersive X-ray (EDX) spectrometry was carried out with a LINK AN 10000 system (Si–Li detector) connected to a JEOL JEM CXII transmission electron microscope operating at 100 kV and equipped with an ASID 4D scanning device (STEM mode). The X-rays emitted from the specimen upon electron impact were collected in the 0–20 keV range for 200–400 s. Atomic compositions (%) were obtained with the 2LINK program (RTS-2/FLS).

The transmission infrared spectra were recorded in the 400–4000 cm^{-1} range at room temperature using a Equinox 55 Bruker FT-IR spectrometer equipped with a DTGS detector. The spectra were taken by averaging 1000 scans, with a scanning velocity of 6.25 Hz and a spectral resolution of 4 cm^{-1}. The spectra were smoothed through the Savitzky–Golay algorithm with a smoothing degree of 13. DTA–TGA measurements were carried out on a SETARAM thermobalance.

The catalytic tests were performed in a 100 ml well-stirred three-phase slurry-type thermoregulated glass reactor containing with 50 ml of a 2 wt.% hexa-1,5-diene solution in heptane. The catalysts (100 mg) were first outgassed for 1 h in the reactor, before treatment with 792 Torr hydrogen at 313 K for 1 h; this procedure was repeated with a final outgassing before introduction of the reaction medium containing the reagent (hexa-1,5-diene), the internal standard (*n*-pentane around 1 wt.%), and the solvent (*n*-heptane), already saturated with hydrogen. Hydrogen was charged up to the operating pressure (792 Torr), while the first analysis sample was collected, and stirring was begun (2000 rpm).

The reaction was carried out at constant pressure, hydrogen being supplied from a thermostated

Table 1
Characteristics of the colloid samples

Sample	Composition	Stabilization	Mean particle size by TEM (nm)	Mean crystallite size by XRD (nm)
COL-PD1	100%Pd	Steric (PVP)	$2.1\left(\frac{\sigma}{d_p}=0.22\right)$	
COL-PD2	100%Pd	Electrostatic (sodium acetate)	$7.0\left(\frac{\sigma}{d_p}=0.2\right)$	5.0
COL-RU1[a]	100%Ru	Electrostatic (sodium acetate)	$1.1\left(\frac{\sigma}{d_p}=0.18\right)$	
COL-RU2[b]	100%Ru	Electrostatic (sodium acetate)		4.5
COL-PDCU	50%Pd/50%Cu	Steric (PVP)	$4.2\left(\frac{\sigma}{d_p}=0.2\right)$	2.9

[a] $C_{acetate} = 3.7 \times 10^{-2}$ mol l^{-1}.
[b] $C_{acetate} = 9.1 \times 10^{-3}$ mol l^{-1}.

vessel, acting as a reservoir, filled initially at 980 Torr.

During the reaction, liquid samples were collected through a syringe valve equipped with a microfilter, at regular H_2 uptake intervals, and analyzed with a Delsi Di200 gas chromatograph (GC) using a flame ionization detector (FID). The reagent (hexa-1,5-diene), the internal standard (*n*-pentane), the solvent (*n*-heptane) and the products (hexane, hex-1-ene, *E*,*Z*-hex-2-ene and *E*,*Z*-hex-3-ene) were separated on a 50 m, 0.2 mm HP PONA capillary column.

The use of standards during the GC analysis allowed the measurement of the concentration of the reactant and of the products cited above. No other byproduct was detected.

3. Results and discussion

3.1. Characterization of the metal colloids

Table 1 collects the characteristics of the samples prepared. For acetate concentrations higher than 10^{-2} mol l^{-1} (COL-RU1), colloidal spherical particles of Ru are obtained (Fig. 1). When the acetate concentration is lower than 10^{-2} mol l^{-1} (COL-RU2),

Fig. 1. TEM micrograph of Ru colloidal particles (COL-RU1).

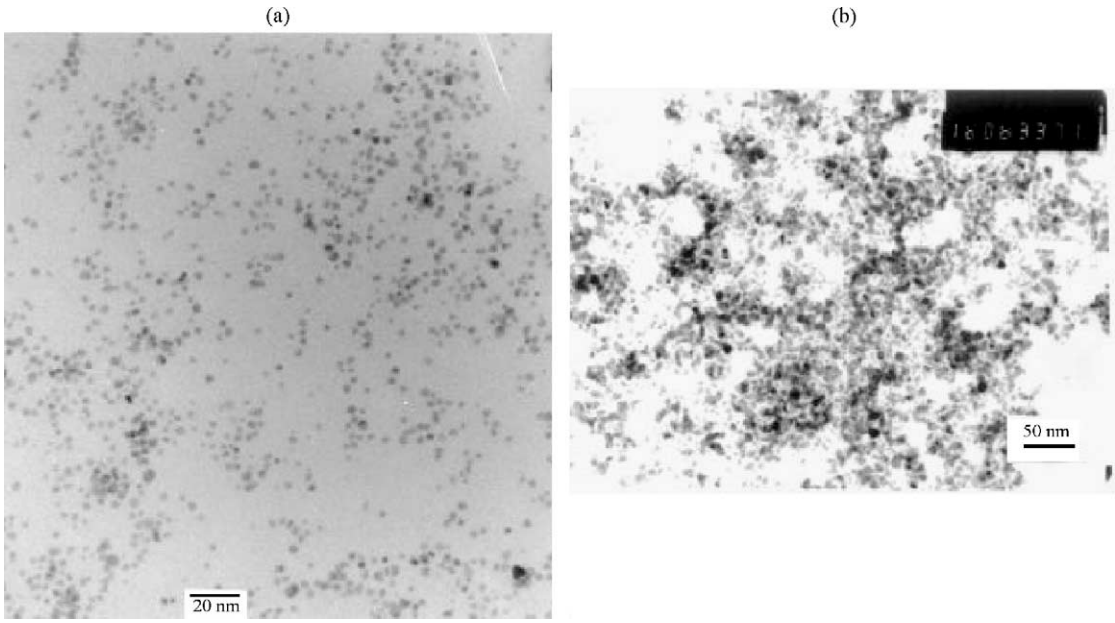

Fig. 2. TEM micrograph of: (a) Pd colloidal particles (COL-PD1), $d_p = 2.0$ nm; (b) PdCu bimetallic colloidal particles (COL-PDCU), $d_p = 4.0$ nm.

the charge repulsion is not strong enough to stabilize the colloidal solution and the particles precipitate due to Van der Waals attraction [16]. Stable Pd and PdCu colloid solutions in liquid polyol were obtained only by adding a protecting PVP polymer (COL-PD1 and COL-PDCU) (Fig. 2). In these latter cases, sodium acetate was not efficient. On the other hand, as the redox potential of light transition metals is lower than that of precious metals, it is more difficult to get metal nanoparticles in the former case [17,18]. PdCu bimetallic particles were prepared with various Pd:Cu ratios and an f.c.c. colloidal solid solution, characterized by a shift of the XRD peaks (between those of Pd and Cu pure materials), was observed for all Pd:Cu concentrations (Fig. 3a). The cell parameters vary linearly with the concentration of the precursors in accordance with Vegard's law [19] (Fig. 3b). In this case, the formation of PdCu nanoparticles involves two steps (Scheme 1): (i) metal hydroxides are formed first by addition of NaOH (pH $\sim$ 10); the color of the solution changed from light-yellow to green, which indicates the formation of bimetallic hydroxide [17]; (ii) the second step is the reduction of the metal hydroxide species by reflux of the solution at

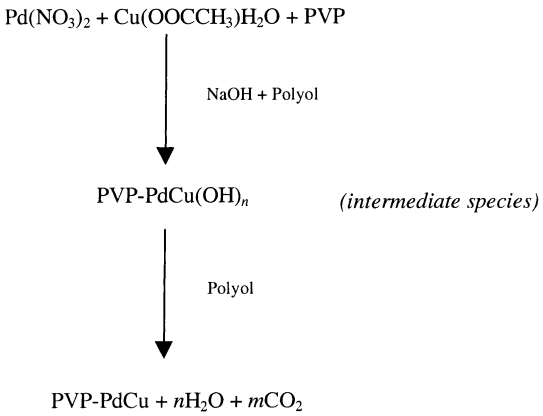

Scheme 1.

198 °C to remove water. After 2 h, the formation of a dark-brown solution of PVP-stabilized PdCu nanoparticles is observed. The polyol oxidation does occur at the same time and the nature of the products formed (glycoaldehyde, glyoxal, glycolic acid, glycoxylic acid, oxalic acid, formic acid and CO_2) depends on the metal precursors [20]. These metal nanoparticles are the parent of the immobilized catalysts.

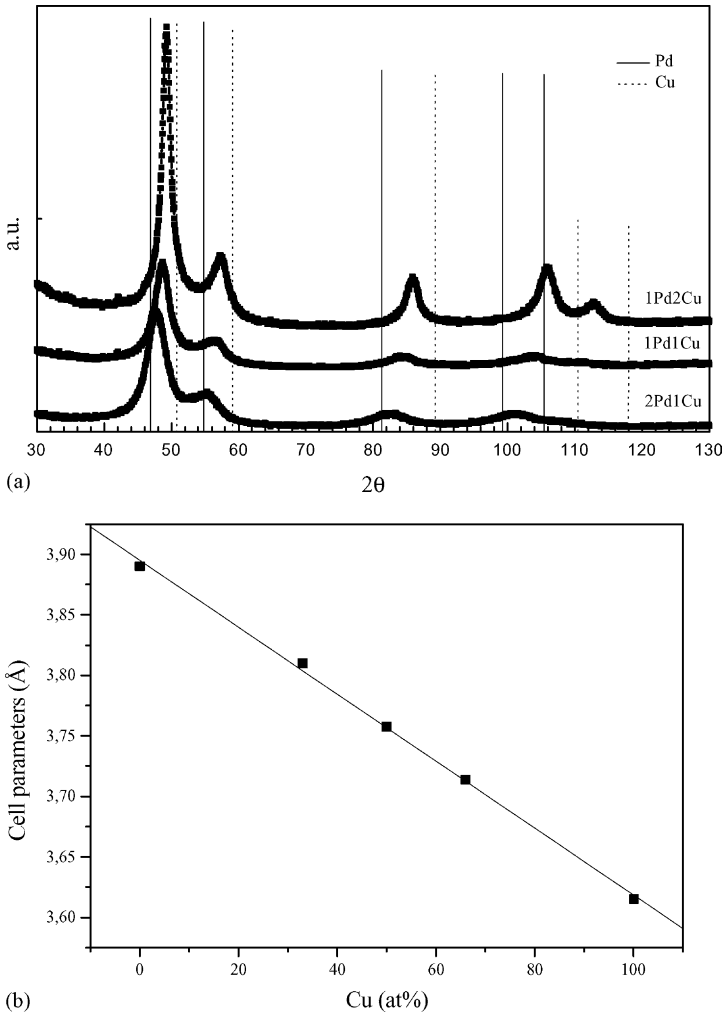

Fig. 3. (a) XRD patterns of colloidal PdCu f.c.c. solid solution; (b) correlation between the cell parameters of PdCu f.c.c. solid solution and the Cu (at.%) concentration.

3.2. Characterization of the immobilized nanoparticles

Table 2 summarized the characteristics of the samples. The immobilization of the colloidal PVP-protected nanoparticles (method 1) was carried out as follows (Fig. 4a): the nanoparticles were precipitated in acetone solution by centrifugation and redispersed in a dichloromethane medium containing γ-MPS or 3-APS to try to exchange the maximum of PVP (adsorbed on the metal particles) with the γ-MPS or 3-APS ligand. After addition of the support, the suspension was vigorously stirred for 48 h at room temperature and then heated at 60 °C for 6 h.

The efficiency of the coordination capture is expected to be determined by the difference in the coordination abilities between the anchored molecules and the PVP.

Method 2 (Fig. 4b) was carried out for the immobilization of the colloid particles prepared by electrostatic stabilization. The bifunctional molecules were anchored on the support via the silane groups before addition of the colloidal solutions; the interaction of the colloidal particles with the grafted

Table 2
Characteristics of immobilized nanoparticles

Sample	Precursor	Composition	d_p by TEM (nm)
MPS-1	COL-PD1	2%Pd/Nb_2O_5	$2.2\left(\frac{\sigma}{d_p}=0.22\right)$
MPS-2	COL-PD2	2%Pd/Nb_2O_5	$7.0\left(\frac{\sigma}{d_p}=0.35\right)$
MPS-3	COL-RU1	2%Ru/Nb_2O_5	$1.3\left(\frac{\sigma}{d_p}=0.15\right)$
MPS-4	COL-RU1	2%Ru/Al_2O_3	$1.2\left(\frac{\sigma}{d_p}=0.15\right)$
MPS-5	COL-PDCU	2%Pd/2%Cu/Nb_2O_5	

support was carried out through vigorous stirring at 60 °C for 6 h.

What is the role of PVP? The average size of the initial (COL-PD1) and immobilized (MPS-1) colloidal particles do not differ significantly (upper part of Tables 1 and 2). In fact, the presence of PVP inhibits the complete adsorption of the bi-coordinating molecules on the metal surface and a PVP-metal film is directly deposed on the oxide. This is supported by the comparison of the transmission electron micrographs of MPS-1 (immobilized PVP-Pd colloid) and of MPS-4 (immobilized Ru colloid prepared without PVP) (Fig. 5). On the latter sample, all metal

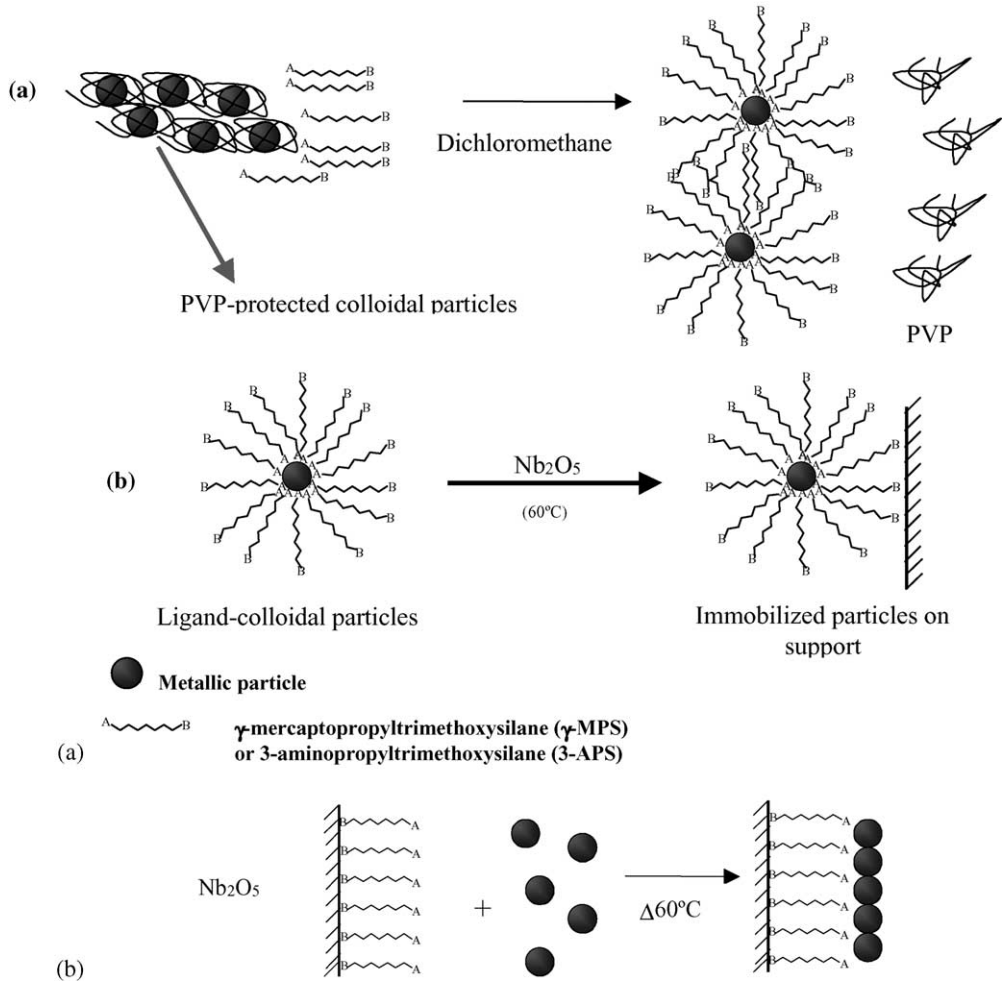

Fig. 4. Immobilization process of colloidal particles: (**a**) method 1; (**b**) method 2.

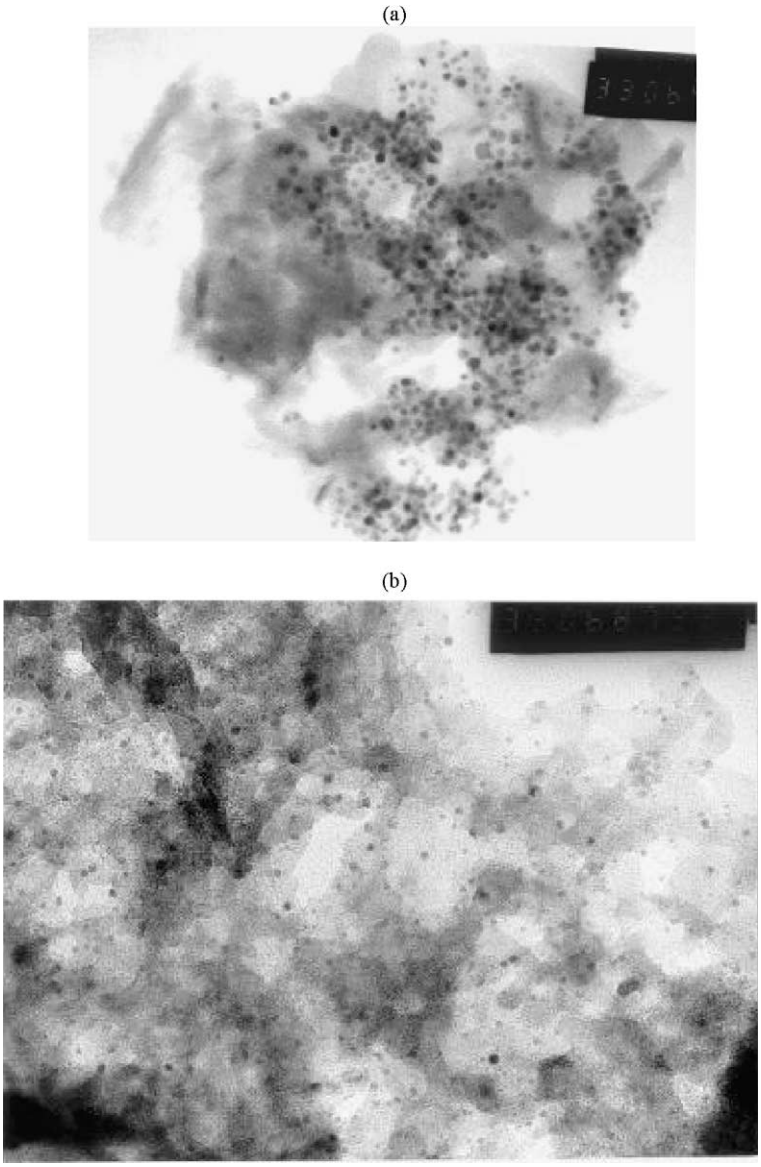

Fig. 5. TEM micrographs of immobilized: (a) PVP-Pd colloid on niobia (MPS-1); (b) Ru colloid on alumina (MPS-4) (see Table 2).

particles are coordinated to MPS and their dispersion on the support is better than on the former. In addition, TGA–DTA analysis of the MPS-4 sample (Fig. 6) shows an endothermic peak at 340 °C accompanied by a mass loss arising from the decomposition of the free S–H containing moiety of γ-MPS (grafted on alumina only) into CO_2 and SO_2. The decomposition of γ-MPS was quantified by EDX measurements (Fig. 7) and a decrease of the sulfur/silicium ratio from 1 to 0.5 was observed. In addition, no sintering of the particles is noticed by STEM analysis (Fig. 8), showing a strong interaction between the bi-coordinating molecule, alumina and metal particles.

Fig. 9 presents the IR spectra of PVP and MPS-1 samples. The ν(CO) stretching vibration is shifted from 1663 cm^{-1} for pure PVP to 1626 cm^{-1} for PVP

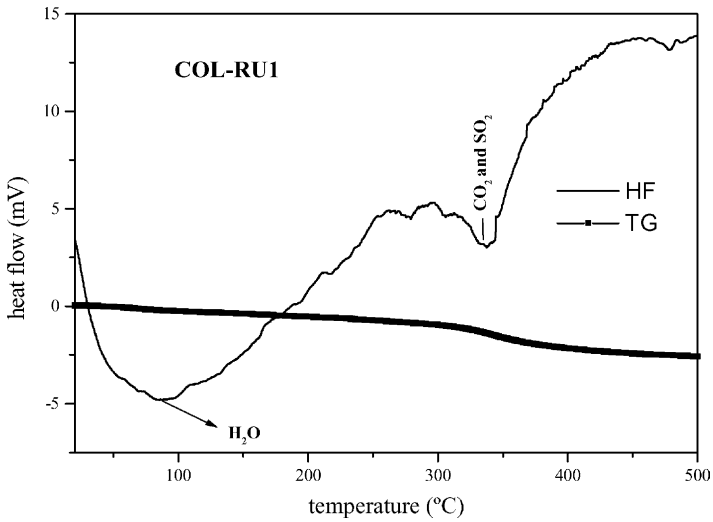

Fig. 6. TGA–DTA analysis of MPS-4 sample.

fixed on Pd particles (Fig. 9). This may result from bond weakening arising from partial electron donation of PVP oxygen to vacant orbitals of palladium surface atoms; this phenomenon was observed for PVP-Ag powders [21]. The presence of PVP after immobilization with γ-MPS on niobia confirms the competition between PVP and the organic molecules (vibrations between 1117 and 880 cm^{-1}) [22], leading to an incomplete immobilization (clear coloration of the filtered solution). The ν(S–H) stretching vibration (2400–2300 cm^{-1}) is also present although partially masked by CO_2 impurity bands.

3.3. Performances in liquid-phase hexa-1,5-diene hydrogenation

The thermodynamic order of stability of the alkene isomers is: *Z*-hex-2-ene > *E*-hex-2-ene > *E*-hex-3-ene > *Z*-hex-3-ene > hex-1-ene [23]. To avoid mass transport limitations, the catalytic tests were performed with: (i) diluted solutions of the reagents (about 2 wt.%), (ii) low catalysts loading (15–100 mg/50 ml), (iii) low reaction temperature (40 °C), and (iv) high stirring rate (ca. 2000 rpm).

Table 3 gives, for each mono- or bimetallic catalyst, the values of: (i) the initial reaction rate (V_s), (ii) the hexa-1,5-diene conversion, (iii) the hex-1-ene selectivity, and (iv) the hex-1-ene productivity. All catalysts present a very good global selectivity S_g (selectivity to hexenes).

Fig. 10 compares the performances of colloidal and immobilized Pd particles; the former (COL-PD1) is PVP-protected with $d_p = 2.1$ nm, and the latter (MPS-2 sample) is obtained ex-acetate-Pd/Nb_2O_5 with $d_p = 7.0$ nm. The PVP-protected samples (MPS-1, MPS-5 and COL-PD1) present an initial induction time (30–50 min) due to the partial elimination of PVP by the solvent (*n*-heptane), not observed for the ex-acetate sample (MPS-2). It was previously shown [24] that the higher catalytic activity results from a compromise between the number of sites and their activity which itself depends on the particle size. For small particle sizes (COL-PD1 and MPS-1), the coordination unsaturation is high and the adsorption of dienes is strong, which decreases the site activity. Conversely, on large particles (MPS-2), the reaction occurs mainly on sites of higher coordination (low unsaturation). These hypotheses are confirmed by the differences in hexa-1,5-diene conversion (Table 3). Similar results were previously reported in the hydrogenation of but-1-yne or butadienes in the liquid phase [25]. On the other hand, when the PVP-Pd colloidal particles were immobilized on the Nb_2O_5 surface, the conversion increases from 30 to 65% and the hex-1-ene productivity from 1.6×10^{-4} to 5.0×10^{-3} mol $s^{-1} g_{metal}^{-1}$ (Table 3),

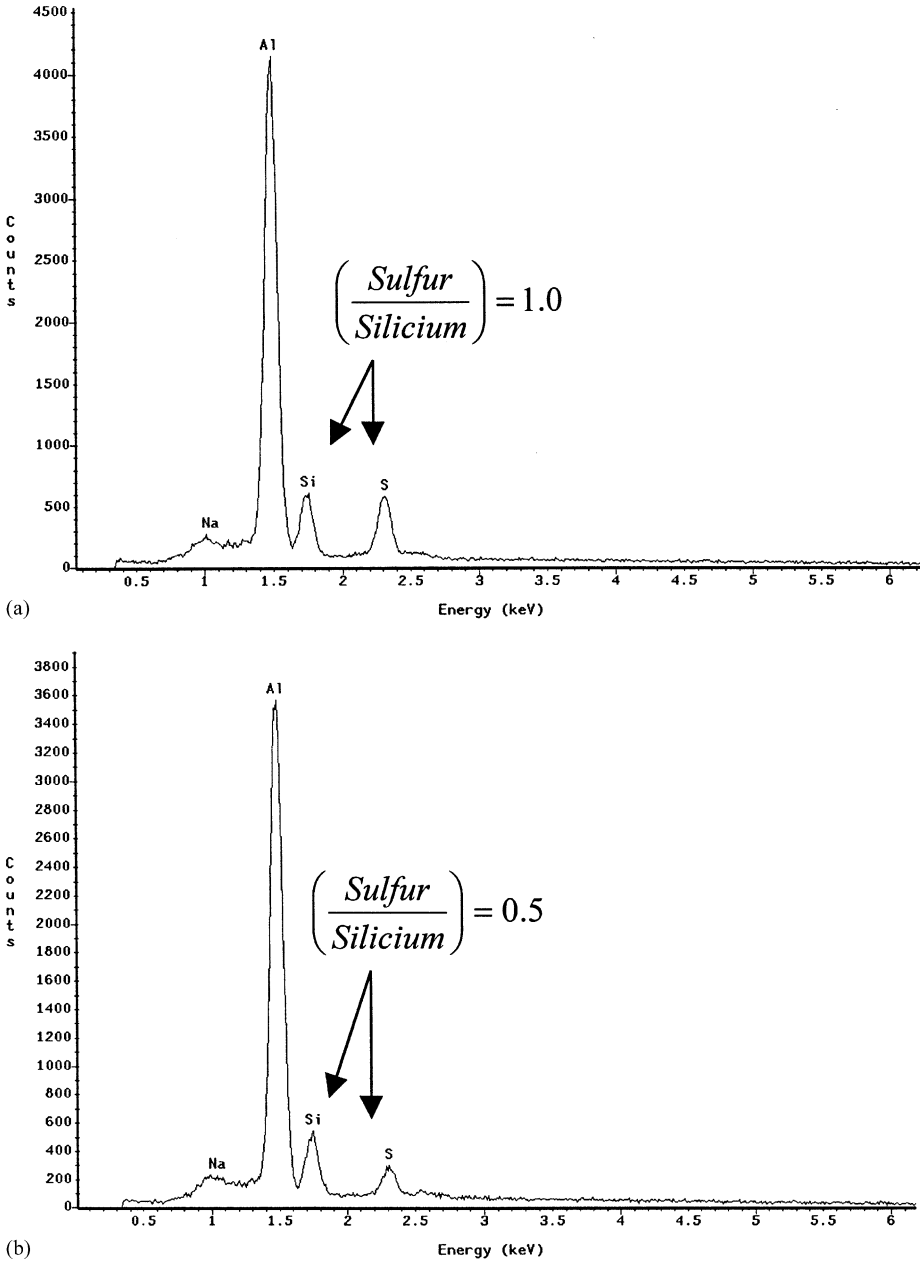

Fig. 7. EDX measurements of MPS-4 sample (a) before and (b) after TGA–DTA analysis.

which shows the efficiency of the immobilization method.

By comparing MPS-5 sample (0.5%Pd/0.5%Cu/Nb_2O_5) with MPS-1, it appears that introduction of Cu leads to a drastic activity decrease and to a marked increase in hex-1-ene selectivity. This can be ascribed to the presence of a PdCu solid solution; in this case, the hydrogenation ability of palladium is modified by

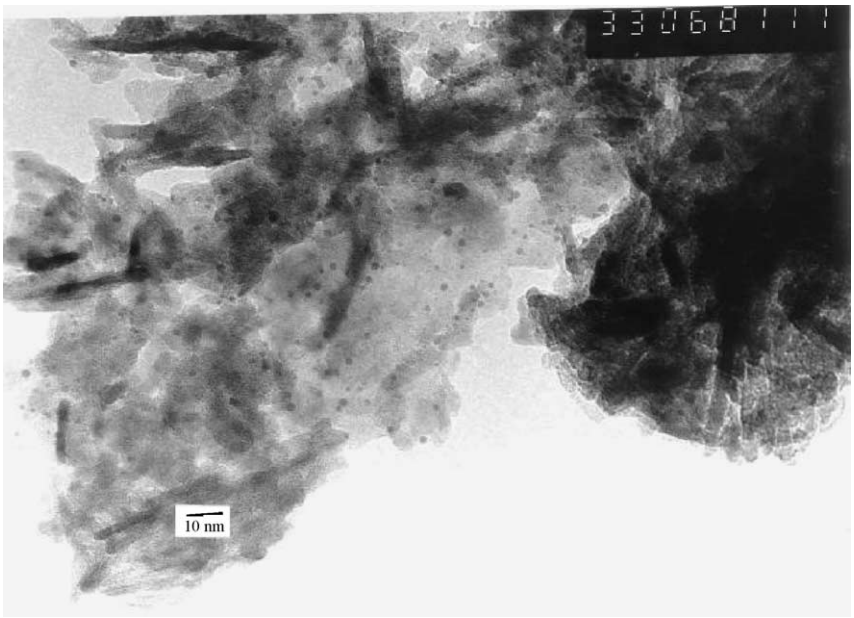

Fig. 8. TEM micrograph of immobilized Ru colloid on alumina (MPS-4) after thermal treatment at 350 °C.

its dilution by copper atoms [26]. This phenomenon was also observed on alumina-supported PdPb alloys in the selective hydrogenation of acetylene [27–29].

According to ICP-AES analysis, the concentration of immobilized metals remains unchanged after catalytic testing, indicating that no active phase leaching occurs.

Finally, the activity and hex-1-ene productivity of immobilized Pd samples are higher than those of unsupported colloidal Pd; in addition, immobilized Ru is less efficient than immobilized Pd; this result may be assigned to: (i) the lower hydrogenation ability of this metal: the activity/selectivity performance order in hydrogenation reactions is Pd > Rh > Pt > Ru > Os > Ir [30,31]; (ii) the high concentration of low coordination sites (smaller particle size).

3.4. Conclusions

The performances of immobilized Pd colloids are better than those of unsupported colloids. This promising method, which avoid direct metal–support interactions, offer new possibilities to control the shape, size and structure of metal nanosized particles in a

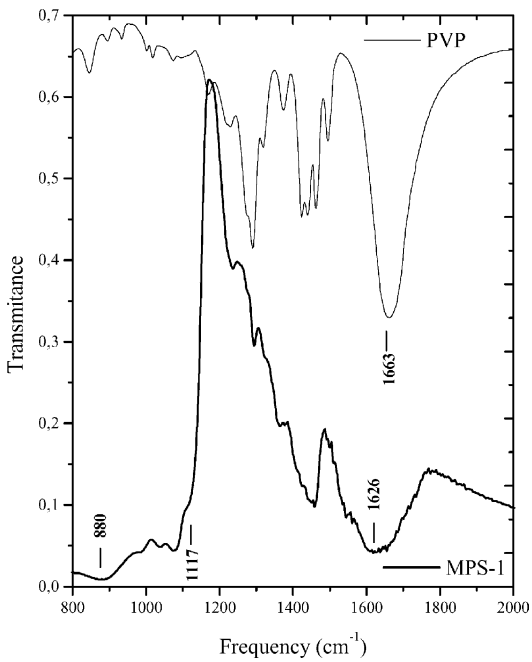

Fig. 9. IR spectra of PVP and 2%Pd/Nb_2O_5 (MPS-1).

Table 3
Catalytic results

Sample	Composition	d_p (nm)	V_s (mol s^{-1} g^{-1}_{metal})[a]	Hexa-1,5-diene conversion (%)	Hex-1-ene selectivity (%)	Hex-1-ene productivity (mol s^{-1} g^{-1}_{metal})
COL-PD1[b]	Colloidal Pd	2.2	2.2×10^{-4}	30	50	1.6×10^{-4}
MPS-1[b]	2%Pd/Nb_2O_5	2.2	5.5×10^{-3}	65	38	5.0×10^{-3}
MPS-2[c]	2%Pd/Nb_2O_5	7.0	8.0×10^{-3}	78	40	6.5×10^{-3}
MPS-3[c]	2%Ru/Nb_2O_5	1.3	5.8×10^{-5}	30	35	2.2×10^{-5}
MPS-5[b]	0.5%Pd/0.5%Cu/Nb_2O_5	4.0	5.2×10^{-4}	20	80	5.0×10^{-4}

[a] Activity (initial rate). The mass of catalysts varied from 15 to 100 mg.
[b] PVP-protected colloidal particles.
[c] Ex-acetate colloidal particles.

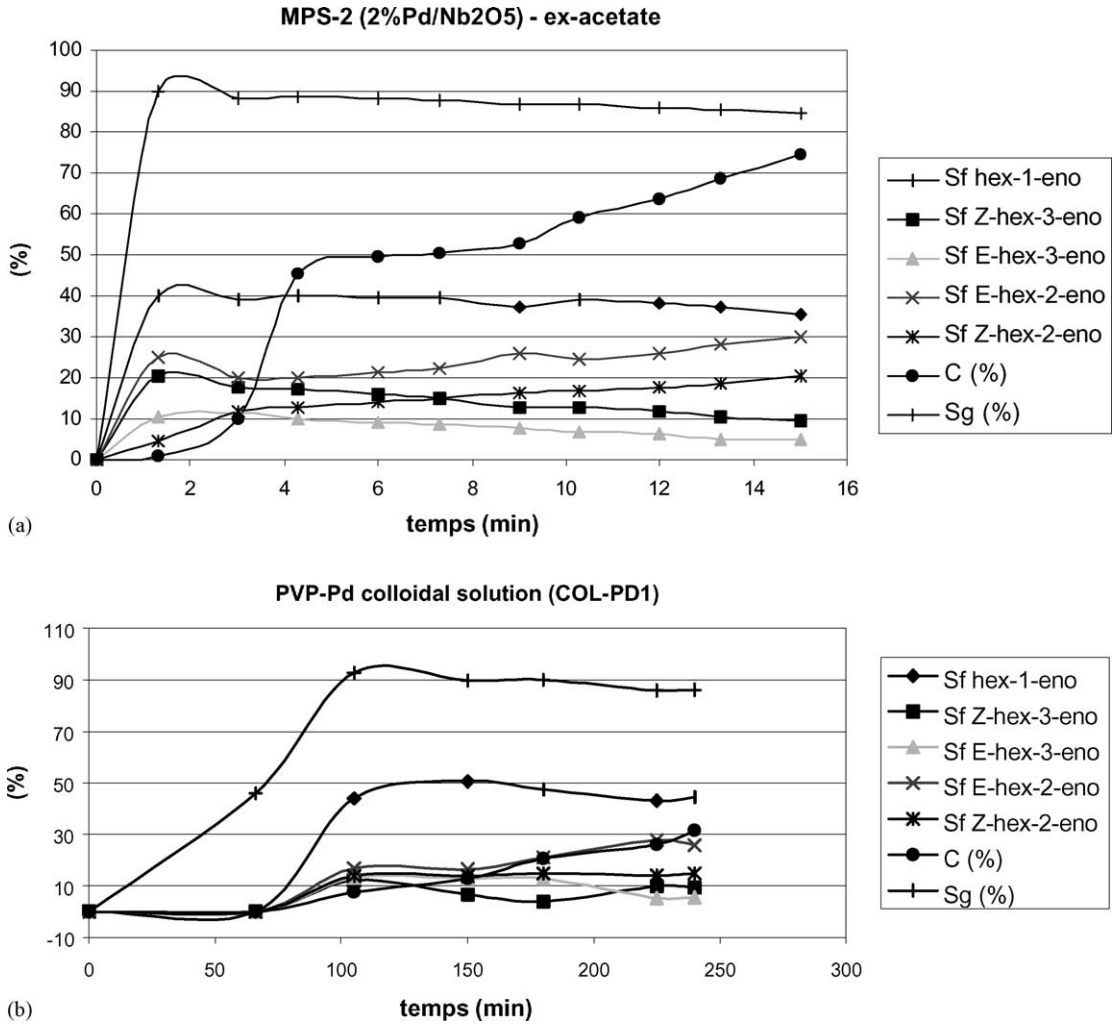

Fig. 10. Global selectivity (S_g), fractional selectivities (S_f) and conversion (C) versus time of: (a) immobilized (MPS-2) and (b) initial (COL-PD1) colloidal samples.

colloidal form, without change upon heterogenation. The present procedure has also been successfully applied to other monometallic (Cu, Pt, Ir, Rh, Ni) and bimetallic (Pd–Cu, Pt–Rh, Ru–Ni) systems. The influence of the nature of the bi-coordinating molecule is now under study.

Acknowledgements

The authors are indebted to CNPq, Brazil, for support and financial resources. Thanks are due to Engelhard-CLAL, France, for Pd and Ru supply. E.A. Sales, Universidade Federal da Bahia, Brazil, is gratefully acknowledged for his help in catalysts testing.

References

[1] G. Schmid, Chem. Rev. 92 (1992) 1709.
[2] J.S. Bradley, E.W. Will, C. Klein, B. Chaudret, A. Duteil, Chem. Mater. 5 (1993) 2540.
[3] H. Hirai, Y. Nakao, N. Toshima, J. Macromol. Sci. Chem. A 13 (1979) 727.
[4] L.N. Lewis, Chem. Rev. 93 (1993) 2693.
[5] A. Elaïssari, Y. Chevalier, F. Ganachaud, T. Delair, C. Pichot, Langmuir 16 (2000) 1261.
[6] E.M.S. Castanheira, J.M.G. Martinho, D. Duracher, M.T. Charreyre, A. Elaïssari, C. Pichot, Langmuir 15 (1999) 6712.
[7] C. Pichot, Th. Delair, A. Elaïssari, NATO ASI Ser. 145 (1997) 515.
[8] M.T. Charreyre, J. Revilla, A. Elaïssari, C. Pichot, B. Gallot, J. Bioactive Compatible Polym. 14 (1999) 64.
[9] D. Duracher, F. Sauzedde, A. Elaïssari, C. Pichot, L. Nabzar, Colloid. Polym. Sci. 276 (1998) 920.
[10] Y. Nakamura, H. Hirai, Chem. Lett. (1986) 1197.
[11] H. Hirai, M. Ohtaki, M. Komiyama, Chem. Lett. (1986) 269.
[12] Y. Wang, H. Liu, Y.X. Huang, Polym. Adv. Technol. 7 (1996) 634.
[13] Q. Wang, H. Liu, H. Wang, J. Colloid. Interf. Sci. 190 (1997) 380.
[14] Y. Nakao, K.J. Kaeriyama, J. Colloid. Interf. Sci. 131 (1989) 186.
[15] P.K. Iler, The Chemistry of Silica, Wiley, New York, 1979.
[16] G. Viau, Ph. Toneguzzo, A. Pierrard, O. Acher, F. Fiévet-Vincent, F. Fiévet, Scripta Mater. 44 (2001) 61.
[17] N. Toshima, in: T. Sugimoto (Ed.), Fine Particles: Synthesis, Characterization and Mechanisms of Growth, Surfactant Science Series, Vol. 92, Marcel Dekker, New York, 2000, p. 430.
[18] F. Fiévet, in: T. Sugimoto (Ed.), Fine Particles: Synthesis, Characterization and Mechanisms of Growth, Surfactant Science Series, Vol. 92, Marcel Dekker, New York, 2000, p. 460.
[19] M. Hansen, K. Anderko, Constitution of Binary Alloys, 2nd Edition, McGraw-Hill, New York, 1985.
[20] B. Blin, F. Fiévet, D. Beaupère, M. Figlarz, New J. Chem. 13 (1989) 67.
[21] Z. Zhang, B. Zhao, L. Hu, J. Solid State Chem. 121 (1996) 105.
[22] B. Mihailova, V. Engström, J. Hedlund, A. Holmgren, J. Sterte, J. Mater. Chem. 9 (1999) 1507.
[23] E.A. Sales, M.J. Mendes, F. Bozon-Verduraz, J. Catal. 195 (2000) 96.
[24] R. Brayner, G. Viau, G.M. Cruz, F. Fiévet-Vincent, F. Fiévet, F. Bozon-Verduraz, Catal. Today 57 (2000) 187.
[25] J.P. Boitiaux, J. Cosyns, S. Vasudevan, Stud. Surf. Sci. Catal. 16 (1983) 123.
[26] R. Brayner, F. Bozon-Verduraz, in press.
[27] H.R. Adúriz, C.E. Gígola, A.M. Sica, M.A. Volpe, R. Touroude, Catal. Today 15 (1992) 459.
[28] J. Goetz, M.A. Volpe, A.M. Sica, C.E. Gigola, R. Touroude, J. Catal. 167 (1997) 314.
[29] M.A. Volpe, P. Rodriguez, C.E. Gigola, Catal. Lett. 61 (1999) 27.
[30] G.C. Bond, G. Webb, P.B. Wells, J.M. Winterbottom, J. Catal. 1 (1962) 74.
[31] M. Boudart, Adv. Catal. 20 (1969) 153.